Available online at www.sciencedirect.com
ScienceDirect
Catalysis Today 119 (2007) 305–310
CATALYSIS TODAY
www.elsevier.com/locate/cattod

Catalytic oxidation of saturated hydrocarbons on multicomponent Au/Al_2O_3 catalysts Effect of various promoters

Andreea C. Gluhoi, Bernard E. Nieuwenhuys *

Department of Heterogeneous Catalysis and Surface Chemistry, Leiden Institute of Chemistry, Leiden University, P.O. Box 9502, 2300 RA Leiden, The Netherlands

Available online 18 September 2006

Abstract

The performance of unpromoted and MO_x-(M: alkali (earth), transition metal and cerium) promoted Au/Al_2O_3 catalysts have been studied for combustion of the saturated hydrocarbons methane and propane. As expected, higher temperatures are required to oxidize CH_4 (above 400 °C), compared with C_3H_8 (above 250 °C). The addition of various MO_x to Au/Al_2O_3 improves the catalytic activity in both methane and propane oxidation. For methane oxidation, the most efficient promoters to enhance the catalytic performance of Au/Al_2O_3 are FeO_x and MnO_x. For C_3H_8 oxidation a direct relationship is found between the catalytic performance and the average size of the gold particles in the presence of alkali (earth) metal oxides. The effect of the gold particle size becomes less important for additives of the type of transition metal oxides and ceria. The results suggest that the role of the alkali (earth) metal oxides is related to the stabilization of the gold nanoparticles, whereas transition metal oxide and ceria additives may be involved in oxygen activation.
© 2006 Elsevier B.V. All rights reserved.

Keywords: Gold; Additives; Promoters; Alkali (earth) metal oxides; Transition metal oxides; Ceria; Methane oxidation; Propane oxidation

1. Introduction

Combustion of hydrocarbons, especially methane, the main component of natural gas requires high temperatures, leading to undesired NO_x formation. Catalytic combustion can lower the temperature and, thus, the emission of NO_x [1–4]. The key to this process is a highly efficient catalyst. Many materials show interesting activity, but very few sustain operation at high temperatures. This is because the activation of the C–H bond in methane requires, besides an active catalyst, relatively high operating temperatures. For longer C–C chains the activation of hydrocarbons becomes easier.

The catalysts that are used can be roughly divided into three groups: noble metal-based catalysts, binary oxides, and mixed oxides with a spinel-like or perovskite-like structure. Among the noble metal-based catalysts, the activity of Pd and Pt catalysts is generally considered to be significantly higher than that of Rh, with palladium (oxide) being the most active. Among transition metal oxides (TMO), the best results were obtained with Co_3O_4 [5,6]. However, Co_3O_4 is not stable at high temperatures [7]. On the other hand, a variety of perovskites may withstand substantially elevated temperatures and with an activity comparable with Pt [2–4,8–10].

It is generally accepted that when transition metal oxides, spinel or perovskites-based catalysts are employed for the total oxidation of hydrocarbons, the oxygen activation step involves the lattice oxygen, viz. nucleophilic oxygen, via a Mars and van Krevelen mechanism [4,11,12].

Since Haruta reported that gold nanoparticles are surprisingly active if prepared and deposited on suitable carriers [13], it is now generally accepted that the special property of catalytically active gold is mainly connected to its particle size which must be in a very narrow range, between 2 nm and 3 nm [14,15], or 3 nm and 5 nm [16–18]. However, an optimum range of 7–8 nm for some reactions has also been claimed [19] and activity has even been reported for particles in the 30–50 nm range [20,21]. Most of the reports agree, however, that for reactions involving CO, hydrocarbons, NO_x and NH_3

* Corresponding author. Tel.: +31 71 527 4545; fax: +31 71 527 4451.
E-mail address: b.nieuwe@chem.leidenuniv.nl (B.E. Nieuwenhuys).

0920-5861/$ – see front matter © 2006 Elsevier B.V. All rights reserved.
doi:10.1016/j.cattod.2006.08.034

molecules, the size of the Au particles should be below 5 nm [22–25].

Gold-based catalysts attracted less interest for CH_4 oxidation, probably because of the high temperature needed to activate this hydrocarbon. However, it was reported that 5% Au/Co_3O_4 is active at very low temperatures, viz. 200–250 °C [26]. Recently, other studies reported on the effect of various transition metal oxides on the catalytic performance of Au/Al_2O_3 [22,27,28].

Results concerning the use of supported Au catalysts for C_3H_8 (total) oxidation are rather scarce. It was reported that Au/Co_3O_4, similar as in methane oxidation, is more active than Pd or Pt supported on Al_2O_3 [29]. Other publications discussed the catalytic activity of Au deposited on Al_2O_3 and CeO_2, but the results were not very encouraging [30]. However, the authors claimed that the co-existence of Au^{3+} and Ce^{4+}, obtained by thermal treatment at 800 °C, is essential for high activity.

This paper presents a study concerning the total oxidation of methane and propane over Au/Al_2O_3 and the effect of various types of additives on the catalytic performance of Au/Al_2O_3 is discussed.

2. Experimental

2.1. Sample preparation

Details of the preparation procedure have been reported elsewhere [25,31,32]. Mixed oxides MO_x/Al_2O_3 were prepared by vacuum impregnation of γ-Al_2O_3 (Engelhard, $S_{BET} = 275\ m^2\ g^{-1}$) with the corresponding $M_x(NO_3)_y$ nitrates (Aldrich > 99.9% purity). After drying for at least 16 h at 80 °C in static air, the samples were subjected to calcination in O_2 flow at 350 °C for 2 h. The prepared mixed oxides typically have an M/Al atomic ratio of 1/15.

Gold was deposited on Al_2O_3 or MO_x/Al_2O_3 via homogeneous deposition-precipitation (HDP) using urea as precipitating agent. The gold precursor used was $HAuCl_4{\cdot}3H_2O$ (Aldrich, 99.99%). The support, the corresponding solution of $HAuCl_4{\cdot}3H_2O$, water and urea in excess were warmed up to 80 °C under vigorous stirring. The final pH of the solution was 8.5. In the next step the slurry was extensively washed with demineralised water in order to remove the Cl^- ions, dried in static air at 80 °C for 16 h and calcined in oxygen flow at 300 °C for 2 h. The intended gold loading was 5 wt.%.

Pt/Al_2O_3 (5 wt.% Pt) was prepared by vacuum impregnation of γ-Al_2O_3 with the corresponding amount of H_2PtCl_6 (Aldrich). After impregnation, the precursor was dried in static air at 80 °C for 16 h and then calcined in oxygen flow at 350 °C.

2.2. Catalyst characterization

The extent of gold deposition on the support loading was determined by means of atomic absorption spectroscopy (AAS) [25,31]. The results are summarized in Table 1.

XRD measurements for the fresh and spent (i.e. after catalytic test) catalysts were carried out using a Philips Goniometer (PW 1050/25) diffractometer equipped with a PW Cu 2103/00 X-ray tube operated at 50 kV and 40 mA. The average gold particle size was estimated from XRD line broadening by using the Scherrer equation. The spectra were recorded between $2\theta = 20^\circ$ and $2\theta = 60^\circ$.

HRTEM measurements were performed using a JEOL 2010 microscope with a point-to-point resolution better than 0.2 nm. The sample was mounted on a carbon polymer supported copper micro-grid. A few droplets of a suspension of the ground catalyst in isopropyl alcohol were placed on the grid, followed by drying at ambient conditions. The average gold particles and the particle size distribution were determined by counting at least 250–300 particles.

2.3. Catalytic activity measurements

The catalytic activity measurements (CH_4 and C_3H_8 total oxidation) have been carried out in a lab-scale fixed bed reactor [25,31]. The samples were reactivated in situ under hydrogen flow at 300 °C. The oxidation of methane was carried out using a reactant ratio $CH_4{:}O_2 = 1{:}4$, and the total oxidation of propane was carried out using a reactant ratio $C_3H_8{:}O_2 = 1{:}16$.

Table 1
The temperature of 50% methane conversion, the specific reaction rate, r (550 °C), the apparent activation energy, E_a, the average size of the gold particles for fresh and spent gold-based catalysts

Catalyst	Au (wt.%)	d^a_{Au} (nm)	d^b_{Au} (nm)	d^c_{Au} (nm)	$T_{50\%}$ (°C)	$r \times 10^3$ (mol CH_4) (mol M)$^{-1}$ s^{-1}	E_a (kJ mol^{-1})
Au/Al_2O_3	4.1 ± 0.1	4.3 ± 0.1	6.0 ± 0.3	5.2 ± 0.3	592	1.7 ± 0.1	74 ± 2
$Au/CeO_x/Al_2O_3$	4.5 ± 0.1	<3.0	5.8 ± 0.3	1.7 ± 0.2	590	1.4 ± 0.2	68 ± 2
$Au/CoO_x/Al_2O_3$	4.3 ± 0.2	5.0 ± 0.1	6.0 ± 0.4	8.0 ± 0.1	580	1.8 ± 0.1	71 ± 3
$Au/FeO_x/Al_2O_3$	4.2 ± 0.2	<3.0	10.2 ± 0.5	n.m.	543	3.0 ± 0.1	70 ± 2
$Au/MnO_x/Al_2O_3$	4.3 ± 0.2	8.0 ± 0.1	14.1 ± 0.6	4.9 ± 0.3	565	2.4 ± 0.2	66 ± 3
$Au/ZnO/Al_2O_3$	4.0 ± 0.1	<3.0	3.9 ± 0.5	n.m.	604	1.4 ± 0.1	79 ± 2
$Au/ZrO_x/Al_2O_3$	3.2 ± 0.1	3.1 ± 0.3	5.5 ± 0.4	n.m.	620	1.5 ± 0.1	82 ± 2
Al_2O_3	–	–	–	–	725	0	120 ± 3
CoO_x/Al_2O_3	–	–	–	–	674	∼0	130 ± 2
FeO_x/Al_2O_3	–	–	–	–	577	0.4 ± 0.1	111 ± 3
MnO_x/Al_2O_3	–	–	–	–	600	0.3 ± 0.1	101 ± 3

M: Au, Co, Fe, Mn, Al. d^a_{Au}: mean diameter of gold particles, as determined by XRD, fresh catalysts (nm). d^b_{Au}: mean diameter of gold particles, as determined by XRD, spent catalysts. d^c_{Au}: mean diameter of gold particles, as determined by HRTEM, fresh catalysts (nm); n.m.: not measured.

All the gases were 4 vol.%/He. The total flow was set to 30 ml min^{-1} (GHSV ~ 1800 h^{-1}). The outlet gas stream was analysed by a mass-spectrometer (Spectra). The reaction cycle consisted of at least two consecutive heating–cooling cycles to a maximum reaction temperature of 750 °C (methane) or 450 °C (propane). Because the total flow and the catalyst weight were always constant (30 ml min^{-1} and 0.2 g), the catalytic performance is compared in terms of the conversion *versus* temperature (second heating cycle) plots. In general the catalysts performed slightly better during the first heating–cooling, cycle but the difference between the cycles did not exceed 30–40 °C. Results obtained during the third or fourth heating cycle were similar to those obtained during the second run. However, the specific reaction rate, *r* (the amount of methane and propane (moles) converted per total amount of Au (moles) and second) was considered as a more precise measure of the catalytic performance, especially because the gold loading was found to vary among the samples.

3. Results

3.1. Methane oxidation

According to the AAS results (Table 1), the gold loading varies between 3.2 wt.% (Au/ZrO_x/Al_2O_3) and 4.5 wt.% (Au/CeO_x/Al_2O_3). Relatively large differences were found in the average size of the gold particles by XRD (d^a_{Au}). The catalysts with MnO_x and CoO_x contain rather large gold particles. However, the gold particles of Au/CeO_x/Al_2O_3 and Au/ZnO/Al_2O_3 were below the detection limit of XRD.

The catalytic performance of unpromoted and MO_x-promoted Au/Al_2O_3 is depicted in Fig. 1 (the results correspond to the second heating stage). Table 1 summarizes the relevant catalytic data in terms of $T_{50\%}$ (temperature needed to convert 50% of methane), the specific reaction rate *r* (550 °C), the variation of the Au particle size before (d^a_{Au}) and after (d^b_{Au}) catalytic reaction and HRTEM results (d^c_{Au}) for some selected fresh catalysts. In addition, the apparent activation energy, E_a, calculated on the basis of the conversion between 0.05 and 0.2 are shown in Table 1. Table 1 also shows the catalytic performance of the most active MO_x/Al_2O_3 samples.

The best promoting effect is obtained with FeO_x as additive. In addition, it is observed that the variation of catalytic activity in methane oxidation is not completely related to the average size of the gold particles, since Au/CeO_x/Al_2O_3 or Au/ZnO/Al_2O_3 are inferior to Au/MnO_x/Al_2O_3, in spite of the very small gold particles for the samples with CeO_x- or ZnO-containing catalysts. If the catalysts are compared on the basis of the *r* variation, the same trend in the ranking order of the catalysts is observed. The addition of Au to various MO_x/Al_2O_3 causes a significant increase of *r*, pointing to the conclusion that Au is the main active component of the catalysts.

The apparent activation energy, E_a strongly decreases by Au addition to Al_2O_3, from 120 kJ mol^{-1} to 74 kJ mol^{-1}. The Arrhenius plots of methane oxidation over Au/Al_2O_3 and Au/CeO_x/Al_2O_3 are shown in Fig. 2A and B. A large number of promoted-Au/Al_2O_3 catalysts have a similar E_a as the unpromoted-Au/Al_2O_3 (i.e. ranging from 70 kJ mol^{-1} to 82 kJ mol^{-1}). The E_a found for Au/MnO_x/Al_2O_3 and Au/CeO_x/Al_2O_3 are slightly lower, as compared with Au/Al_2O_3

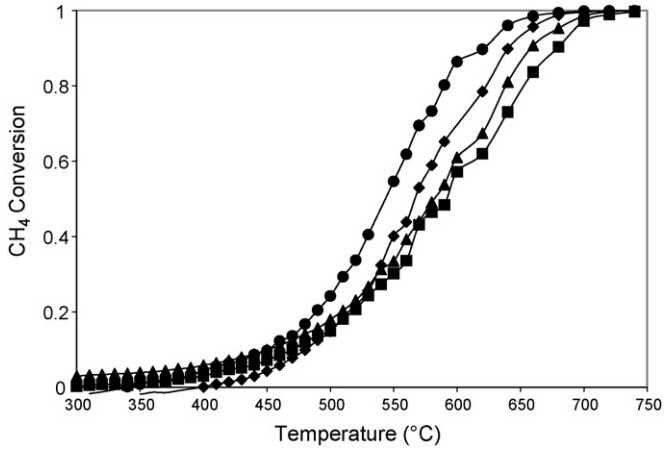

Fig. 1. Methane conversion *vs*. temperature over Au/Al_2O_3 (■), Au/CoO_x/Al_2O_3 (▲), Au/MnO_x/Al_2O_3 (◆), Au/FeO_x/Al_2O_3 (●). Reactant ratio: CH_4:O_2 = 1:4.

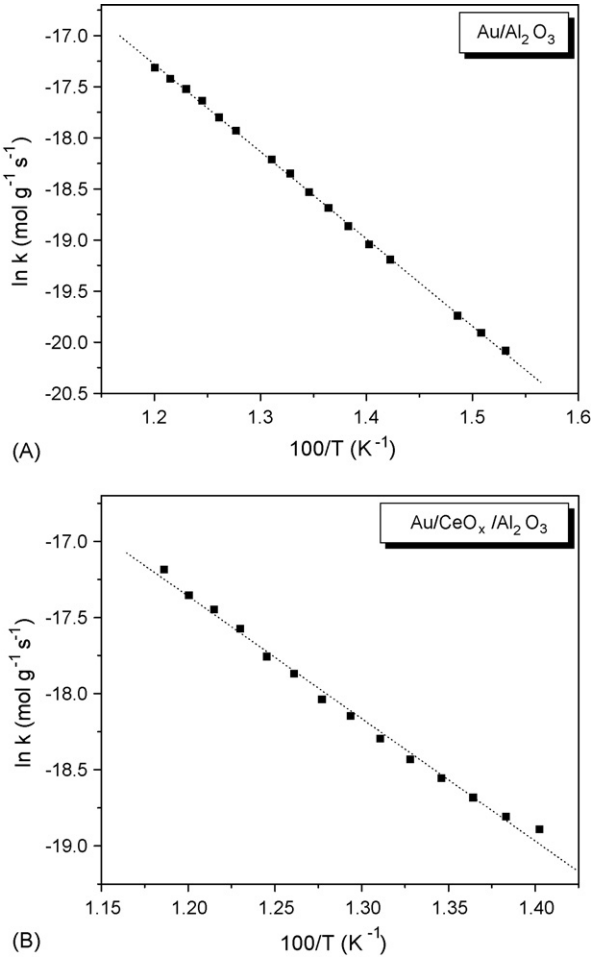

Fig. 2. Arrhenius plots of methane oxidation over Au/Al_2O_3 (A) and Au/CeO_x/Al_2O_3 (B).

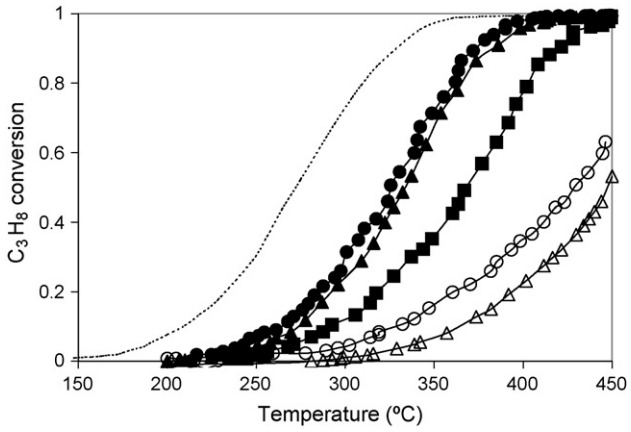

Fig. 3. Propane oxidation *vs.* temperature over Au/Al_2O_3 (△), $Au/BaO/Al_2O_3$ (○), $Au/FeO_x/Al_2O_3$ (■), $Au/CoO_x/Al_2O_3$ (▲), $Au/MnO_x/Al_2O_3$ (●), Pt/Al_2O_3 (–). Reactant ratio C_3H_8:O_2 = 1:16.

(66 kJ mol^{-1} and 68 kJ mol^{-1}). On the other hand, the E_a of the all MO_x/Al_2O_3 tested is above 100 kJ mol^{-1}.

Regarding the stability of the gold particles during the methane oxidation test, rather significant sintering was found by XRD. This is expected, since the temperature used is quite high and exceeds by far the Tamman temperature of Au. However, some of the catalysts appear less affected by the temperature, probably because for those catalysts the additives work more efficiently as structural promoters.

3.2. Propane oxidation

Fig. 3 illustrates the changes in the catalytic activity of Au/Al_2O_3 after addition of various additives such as BaO, TM (Fe, Mn, Co) oxides and ceria. The figure also compares the catalytic activity of various gold-based catalysts with that of Pt/Al_2O_3 (5 wt.% Pt). Among the gold-containing catalysts, the most efficient one contains MnO_x as additive. Obviously, this high catalytic activity is not critically related to the average size of the gold particles, around 8 nm (Table 2). Almost the same degree of C_3H_8 conversion is obtained over $Au/CoO_x/Al_2O_3$. FeO_x- and CeO_x-containing Au/Al_2O_3 are slightly less active, but still superior to samples with TiO_x or VO_x as additives, i.e. catalysts which contain very small Au particles. The results indicate that for all the Au-based catalysts, small Au particles are not sufficient to obtain high activity. However, the most active Au-based catalyst is still inferior to Pt/Al_2O_3.

All the relevant data ($T_{50\%}$, r, E_a and the variation of the size of the gold particles after the catalytic reaction) are summarized in Table 2. More than a six-fold increase of the specific reaction rate, r, calculated at 370 °C, is found after MnO_x addition to Au/Al_2O_3.

Similar as for methane oxidation, the addition of Au to Al_2O_3 decreases the apparent activation energy. The E_a is in the same range as found for CH_4. For the MO_x-promoted Au/Al_2O_3 catalysts, the apparent activation energy resembles the value found for Au/Al_2O_3. The apparent activation energies of the MO_x/Al_2O_3 are larger than the E_a of $Au/MO_x/Al_2O_3$. The apparent activation energy of Pt/Al_2O_3 is much lower than for the gold-based catalysts, around 68 kJ mol^{-1}, in line with previously reported results [33].

According to the XRD results, sintering of the gold nanoparticles does not proceed significantly under the experimental conditions used.

4. Discussion

C–H bond activation in saturated hydrocarbons is a crucial step in the combustion of these compounds [4,11,12,34]. Once the first bond is broken, sequential reactions to CO_2 and H_2O are more facile. Methane is the most difficult hydrocarbon to activate, and propane activation is of intermediate difficulty [35]. This activation is also partly related to the ease of adsorption of these hydrocarbons. An important factor is the

Table 2
The temperature of 50% C_3H_8 conversion, the specific reaction rate, r (370 °C), the apparent activation energy, E_a, the average size of the gold particles for fresh d^a_{Au} and spent (after reaction) d^b_{Au} gold-based catalysts (XRD)

Catalyst	Au (wt.%)	d^a_{Au} (nm)	d^b_{Au} (nm)	$T_{50\%}$ (°C)	$r \times 10^4$ (mol C_3H_8) (mol M)$^{-1}$ s^{-1}	E_a (kJ mol^{-1})
Au/Al_2O_3	4.1 ± 0.1	4.3 ± 0.1	5.1 ± 0.4	447	1.7 ± 0.1	81 ± 1
$Au/Li_2O/Al_2O_3$	4.0 ± 0.3	3.2 ± 0.1	4.3 ± 0.4	450	1.3 ± 0.1	80 ± 2
$Au/Rb_2O/Al_2O_3$	3.5 ± 0.1	<3.0	3.8 ± 0.2	430	3.5 ± 0.1	75 ± 2
$Au/BaO/Al_2O_3$	3.6 ± 0.2	<3.0	4.1 ± 0.1	423	3.3 ± 0.2	74 ± 3
$Au/MnO_x/Al_2O_3$	4.3 ± 0.2	8.0 ± 0.1	9.2 ± 0.1	325	11.3 ± 0.2	81 ± 1
$Au/CoO_x/Al_2O_3$	4.3 ± 0.2	5.0 ± 0.1	5.5 ± 0.2	333	10.3 ± 0.1	83 ± 2
$Au/CeO_x/Al_2O_3$	4.5 ± 0.1	<3.0	3.4 ± 0.3	372	7.2 ± 0.1	75 ± 1
$Au/FeO_x/Al_2O_3$	4.2 ± 0.2	<3.0	3.6 ± 0.5	368	6.4 ± 0.1	80 ± 2
$Au/PrO_x/Al_2O_3$	3.9 ± 0.1	3.0 ± 0.3	3.2 ± 0.3	401	3.6 ± 0.1	78 ± 2
$Au/TiO_x/Al_2O_3$	4.1 ± 0.1	<3.0	3.7 ± 0.4	419	2.7 ± 0.1	78 ± 1
$Au/VO_x/Al_2O_3$	4.3 ± 0.2	<3.0	3.3 ± 0.2	419	1.5 ± 0.1	83 ± 1
$Au/ZrO_x/Al_2O_3$	4.0 ± 0.1	3.1 ± 0.3	3.9 ± 0.1	450	2.1 ± 0.1	85 ± 2
$Au/YO_x/Al_2O_3$	4.1 ± 0.2	<3.0	3.8 ± 0.6	384	5.3 ± 0.2	82 ± 2
Pt/Al_2O_3	–	–	–	274	10.7 ± 0.2	68 ± 1
Al_2O_3	–	–	–	>450	0	112 ± 2
MnO_x/Al_2O_3	–	–	–	359	0.7 ± 0.1	120 ± 2
CoO_x/Al_2O_3	–	–	–	365	2.4 ± 0.2	101 ± 3

M: Au, Pt, Mn, Co, Al.

"stickiness" of the molecules to a metallic or oxidized surface. Since the C–H bond in methane is only very weakly acidic ($pK_a = 46$), the surface sites capable of deprotonation of methane must be very basic. However, such sites would be expected to adsorb CO_2 rather strongly, and so they might be expected to be rapidly self-poisoned [34]. Besides the basic sites, also the acidic sites were proposed as important for saturated hydrocarbon oxidation [36]. All these models are, however, based on metal oxide-like catalysts. If the catalyst is a metal-based catalyst, the rate of activation of the C–H bond depends on the nature of the hydrocarbon, the nature of the metal, and the reaction conditions. In general the surface composition of a metal catalyst depends on the reaction conditions and varies from more oxidized surface (oxygen-rich conditions) to more reduced surface (fuel-rich conditions). For methane oxidation, it is well established that Pd is the most active catalyst, but that Pt is a better catalyst for the oxidation of higher hydrocarbons [37,38]. On the other hand, Haruta reported that Au deposited on Co_3O_4 is more efficient in total oxidation of the saturated hydrocarbons than Pt or Pd deposited on alumina [39]. However, those results were obtained using a large difference in the loading of the active metal, 10 wt.% Au (Au/Co_3O_4) and 1 wt.% Pt and Pd (Pt/Al_2O_3 and Pd/Al_2O_3). Our results clearly confirm that Pt/Al_2O_3 is superior to any of the gold-based catalysts for a similar loading of the noble metal.

The results presented in this paper show that the oxidation of methane and propane over gold-based catalysts is related to the size of the gold particles, but this is not the only effect that controls the catalytic activity. An illustration of the dependence of the $T_{50\%}$ with the average gold particle size is presented in Fig. 4A and B for methane and propane oxidation. Methane conversion is related to the size of the gold particles, but also to the identity of the MO_x. A more pronounced effect of the additives on the catalytic performance of Au/Al_2O_3 is observed for propane oxidation (Fig. 4B). Only the alkali (earth) metal oxide containing catalysts exhibit a direct dependence of the catalytic performance with the size of Au particles. Moreover, in the presence of these additives the growth of the Au particles during calcination and catalytic process appears to be retarded [25,31]. For the other samples, a gold particle size of ~3 nm is particularly important for a high catalytic activity, next to the identity of the additive.

The anomalous effects observed for both methane and propane oxidation and the absence of correlation between activity and particle size could be attributed to the metal–support interaction. A stronger metal–support interaction affects the geometry/structure of the Au nanoparticles. Thus, the Au nanoparticles may change their shape from spherical to flat. Flat Au particles are reported to be more active [40]. Moreover, TMO and ceria contain an increased number of defects, useful as anchoring sites for Au. However, it should be mentioned that based on the HRTEM micrographs, there is no direct correlation between the catalytic activity in saturated hydrocarbons oxidation and a particular shape of the gold particles.

Moreover, the additives that are most probably directly responsible for the existence of a certain metal–support

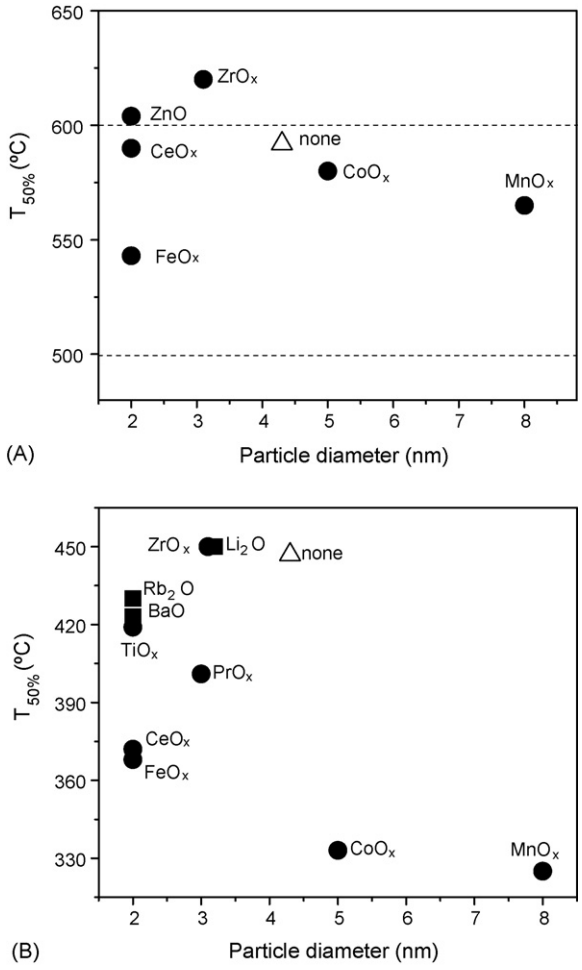

Fig. 4. $T_{50\%}$ *vs.* particle diameter for methane (A) and propane (B) oxidation (XRD results). For the catalysts with Au particle size below 3.0 nm, an arbitrary value of 2.0 nm was considered.

interaction also contribute to the availability of surface oxygen and its overall mobility. The presence of MO_x (MO_x: TMO and ceria) seems essential for the fast and complete oxidation. Although at sufficiently high temperatures the catalytic oxidation takes place even on catalysts with non-redox couple oxides, for example $Au/BaO/Al_2O_3$, the presence of M^{n+} with strong redox capacity is more beneficial. The overall reaction rate may be controlled either by the activation of the C–H bond, or by the reoxidation of $M^{(n-1)+}O_x$ to $M^{n+}O_x$. The activation of the C–H bond appears to be directly related to the presence of Au, whereas the availability of appropriate oxygen species is connected to the identity of $M^{n+}O_x$. The two different processes (C–H bond activation and oxygen activation) may also explain the difference found in E_a for both oxidation reactions. After Au addition to Al_2O_3 the apparent activation energy decreases drastically. This decrease implies that Au plays an active role in the activation of these hydrocarbons. Grisel reported similar results for methane oxidation over Au-based catalysts [22,27,28]. A similar model as the one already published for methane oxidation over Pd/Al_2O_3 [38] was used to explain the results obtained for Au/Al_2O_3 [28]: the E_a was seen as an "average value" on the basis of different Au particles, with

variable size. This is a reasonable suggestion, since it is known that smaller Au particles have an increased number of kinks and steps where the activation of various molecules is more likely to proceed. Larger Au particles, on the other hand, resemble the characteristics of inactive bulk-Au.

Similar results have also been earlier reported for Au-based catalysts promoted with ceria, TMO and alkali (earth) metal oxides for total oxidation of propene [25,31]. It was found that the lattice oxygen of CeO_x and MnO_x is directly involved in the oxidation of propene and that lower temperatures are required to activate propene, compared with methane and propane.

In addition, some relationship between the catalytic activity and the acid/base character of the additives may exist. Thus, if the additive has a relatively strong acidic character, such as VO_x, the catalytic performance in C_3H_8 oxidation is very low. However, most of the oxides used as additives have a basic character (Lewis acid), which varies from weak (Al_2O_3) to strong or very strong (MgO, BaO, NiO, CuO, ZnO). Moreover, the basic strength of the MO_x does not reflect the variation in the catalytic performance. Thus, an oxide with a medium-weak basic character such as FeO_x appears to have a more pronounced effect on the activity of Au/Al_2O_3 than a medium-strong (ZrO_x) or very strong (BaO) oxide. Oxides with a basic character are beneficial, compared with those with an acidic character. This model would be important, however, if these additives are directly involved in the activation of the hydrocarbon. If their role is, as already discussed, rather to supply active oxygen, then their acid/base character is less important. More probably, the hydrocarbons are activated on gold or at the Au–support interface, whereas oxygen is activated/supplied by the mixed support.

5. Conclusions

The significant decrease of $T_{50\%}$ and E_a, accompanied by an increase in r after addition of Au to MO_x/Al_2O_3 indicates that Au is the active species in the oxidation of saturated hydrocarbons such as methane and propane. The results show that a direct relationship exists between the catalytic performance and the average size of the Au particles, especially in the presence of alkali (earth) metal oxide additives. Their role is probably that of a structural promoter. On the other hand, if the additives are of the type of transition metal oxides and ceria, the size of Au particles does not seem to be that crucial anymore. These additives may function as a cocatalyst, i.e. as supplier of oxygen. Promising catalysts for propane oxidation are those with BaO or Rb_2O as promoters. However, the efficiency of the Au-based catalysts can be even further improved if oxides such as MnO_x, FeO_x, CoO_x or CeO_x are added.

Regarding the stability of the gold nanoparticles in propane oxidation, the presence of the additives prevents their sintering even during an extended period in the reactor. However, the temperatures needed to activate CH_4 are rather high for very small Au particles and growth of these particles is observed.

References

[1] R. Prasad, L.A. Kennedy, E. Ruckenstein, Catal. Rev. Sci. Eng. 26 (1984) 1.
[2] M.F.M. Zwinkels, S.G. Jaras, P.G. Menon, T.A. Griffin, Catal. Rev. Sci. Eng. 35 (1993) 319.
[3] R.A. Dalla Betta, Catal. Today 35 (1997) 129.
[4] M. Alifanti, J. Kirchnerova, B. Delmon, D. Klvana, Appl. Catal. A 262 (2004) 167.
[5] J.E. Germain, Catalytic Conversion of Hydrocarbons, Academic Press, 1967.
[6] G.K. Boreskov, in: J.R. Anderson, M. Boudart (Eds.), Catalysis, Science and Technology, vol. 3, Springer Verlag, New York, 1982, p. p39.
[7] E. Garbowski, M. Guenin, M.C. Marion, M. Primet, Appl. Catal. 64 (1990) 209.
[8] S. Royer, F. Berube, S. Kaliaguine, Appl. Catal. A 282 (2005) 273.
[9] N. Yi, Y. Cao, Y. Su, W.L. Dai, H.Y. He, K.N. Fan, J. Catal. 230 (2005) 249.
[10] V.V. Kharton, A.A. Yaremchenko, A.A. Valente, V.A. Sobyanin, V.D. Belyaev, G.L. Semin, S.A. Veniaminov, E.V. Tsipis, A.L. Shaula, J.R. Frade, J. Rocha, Solid State Ionics 176 (2005) 781.
[11] G. Busca, M. Daturi, E. Finocchio, V. Lorenzelli, G. Ramis, R.J. Wiley, Catal. Today 33 (1997) 239.
[12] G. Busca, E. Finocchio, G. Ramis, G. Ricchiardi, Catal. Today 32 (1996) 133.
[13] M. Haruta, T. Kobayashi, N. Yamada, Chem. Lett. 2 (1987) 405.
[14] D.T. Thompson, Gold Bull. 32 (1999) 12.
[15] M. Valden, X. Lai, D.W. Goodman, Science 281 (1998) 1647.
[16] G.C. Bond, Gold Bull. 34 (2001) 117.
[17] B.E. Salisbury, W.T. Wallace, R.L. Whetten, Chem. Phys. 262 (2000) 131.
[18] D.T. Thompson, Gold Bull. 31 (1998) 111.
[19] L. Prati, G. Martra, Gold Bull. 32 (1999) 96.
[20] Y. Yuan, A. Kozlova, H. Asakura, H. Wan, K. Tsai, Y. Isawa, J. Catal. 170 (1997) 191.
[21] H.S. Oh, J.H. Yang, C.K. Costello, Y.M. Wang, S.R. Bare, H.H. Kung, M.C. Kung, J. Catal. 210 (2002) 375.
[22] R.J.H. Grisel, B.E. Nieuwenhuys, Catal. Today 64 (2001) 69.
[23] M. Haruta, CATTECH 6 (2002) 102.
[24] G.C. Bond, D.T. Thompson, Catal. Rev. Sci. Eng. 41 (1999) 319.
[25] A.C. Gluhoi, N. Bogdanchikova, B.E. Nieuwenhuys, J. Catal. 229 (2005) 154.
[26] R.D. Waters, J.J. Weimer, J.E. Smith, Catal. Lett. 30 (1995) 181.
[27] R.J.H. Grisel, P.J. Kooyman, B.E. Nieuwenhuys, J. Catal. 191 (2000) 430.
[28] R.J.H. Grisel, Supported gold catalysts for environmental applications, PhD Thesis, Leiden University, 2002.
[29] M. Haruta, Now and Future 7 (1992) 13.
[30] P. Bera, M.S. Hegde, Catal. Lett. 79 (2002) 75.
[31] A.C. Gluhoi, N. Bogdanchikova, B.E. Nieuwenhuys, J. Catal. 232 (2005) 96.
[32] A.C. Gluhoi, M.A.P. Dekkers, B.E. Nieuwenhuys, J. Catal. 219 (2003) 197.
[33] T.F. Garetto, E. Rincon, C.R. Apesteguia, Appl. Catal. B 48 (2004) 167.
[34] R. Burch, D.J. Crittle, M.J. Hayes, Catal. Today 47 (1999) 229.
[35] T.V. Choudhary, S. Banerjee, V.R. Choudhary, Appl. Catal. A 234 (2002) 1.
[36] V.R. Choudhary, V.H. Rane, J. Catal. 130 (1991) 411.
[37] F.H. Ribeiro, M. Chow, R.A. Dalla Betta, J. Catal. 146 (1994) 537.
[38] R.F. Hicks, H.H. Qi, M.L. Young, R.G. Lee, J. Catal. 122 (1990) 280.
[39] M. Haruta, Catal. Today 36 (1997) 153.
[40] N. Lopez, J.K. Norskov, T.V.W. Janssens, A. Carlsson, A. Puig-Molina, B.S. Clausen, J.D. Grunwaldt, J. Catal. 225 (2004) 86.